

Quantum transport phenomena and their modeling

Frederik O. Heinz, Fabian M. Bufler, Andreas Schenk and Wolfgang Fichtner

Institut für Integrierte Systeme, ETH Zürich, CH-8092 Zürich, Switzerland
e-mail: frederik.heinz@iis.ee.ethz.ch

Abstract

The physical foundations of the received models in semiconductor device modeling are reviewed, and their limitations for the simulation of small devices are discussed. The limitations result from non-local effects. These may be classified into *classical non-localities*, that arise far from equilibrium, and *quantum-mechanical non-localities*, that result from the wave nature of the charge carriers. In this paper we discuss simulation strategies capable of addressing both types of non-localities.

Keywords: non-local effects, (quasi-)ballistic transport, quantum-coherent transport, 2D/3D quantum effects

1 Introduction

The exponential growth of the number of transistors per integrated circuit (IC) predicted by Moore's law [1] is accompanied by a steady reduction of the size of each individual transistor. For decades each IC generation could be derived from the previous one by simple scaling of device geometry and voltages, the only limiting factor being process technology. For the year 2016, the International Technology Roadmap for Semiconductors [2] predicts a physical gate length of 9 nm for both logic and memory applications. Thus, scaling eventually will reduce the extensions of semiconductor devices to sizes at which some of the assumptions underlying scaling, *e.g.* the *locality of transport parameters*, break down.

In order to assess the implications of the ongoing down-scaling for the simulation of semiconductor devices it is essential to be aware of the physical foundations of the models employed by the simulation software and of the assumptions made in deriving them.

In this paper we will review the received models in present day device simulation, discuss their limitations, and suggest methods to overcome them. The discussion covers MOSFETs on the whole range from present day devices down to hypothetical nano-MOSFETs operating in the quantum-coherent transport limit. Other device types that will be discussed comprise Coulomb blockade devices with quantum confinement and hybrid devices with both dissipative channels *and* quantum dots.

2 Transport models in device simulation

2.1 Classical models

The most commonly employed models in semiconductor device simulation are based on the classical Boltzmann transport equation (BTE) [3]

$$\left(\frac{\partial}{\partial t} + \mathbf{v} \cdot \nabla_{\mathbf{r}} + \mathbf{F} \cdot \nabla_{\mathbf{p}} \right) f(\mathbf{r}, \mathbf{p}, t) = \underbrace{\sum_{\mathbf{p}'} (S(\mathbf{p}', \mathbf{p})f(\mathbf{r}, \mathbf{p}', t) - S(\mathbf{p}, \mathbf{p}')f(\mathbf{r}, \mathbf{p}, t))}_{=:(df/dt)_{\text{coll}}}. \quad (1)$$

Here, f is the classical distribution function

$$f(\mathbf{r}, \mathbf{p}, t) d^3r d^3p = \#(\text{particles in } d^3r d^3p), \quad (2)$$

and $(df/dt)_{\text{coll}}$ denotes its change over time due to collisions. The Boltzmann equation originally was used to study the thermal properties of classical gases. A few alterations are necessary to adapt it to the computation of charge carrier transport in semiconductor devices:

- momentum \mathbf{p} : needs to be replaced by the *crystal momentum* $\mathbf{p}_{\text{crystal}}(\mathbf{k}) = \hbar\mathbf{k}$.
- velocity \mathbf{v} : use the velocity expectation value of a Bloch wavefunction of wave vector \mathbf{k}

$$\mathbf{v}(\mathbf{k}) := \frac{1}{\hbar} \nabla_{\mathbf{k}} \tilde{\epsilon}(\mathbf{k}), \quad (3)$$

where $\tilde{\epsilon}$ is the band dispersion relation [4].

- scattering rates S : use the quantum-mechanical transition probabilities per unit time.
- Pauli exclusion principle: in a scattering process, the final state must be unoccupied.

$$f(\mathbf{r}, \mathbf{k}', t) \rightsquigarrow f(\mathbf{r}, \mathbf{k}', t)(1 - f(\mathbf{r}, \mathbf{k}, t)), \quad (4)$$

$$f(\mathbf{r}, \mathbf{k}, t) \rightsquigarrow f(\mathbf{r}, \mathbf{k}, t)(1 - f(\mathbf{r}, \mathbf{k}', t)). \quad (5)$$

Except for quantum-mechanical non-localities, all characteristics of a semiconductor device may be inferred by solving the Boltzmann equation.

2.1.1 The method of moments

The usual models in device simulation, such as the drift–diffusion, energy balance or the hydrodynamic model, all are variants of the *method of moments* [5] for the solution of the Boltzmann equation. Solving the full Boltzmann equation (1) requires great computational effort: it is an integro–differential equation for a distribution $f(\mathbf{r}, \mathbf{k}, t)$ over \mathbb{R}^7 ; furthermore, the exact collision term is inapproachable by standard discretisation schemes. To speed up procedures, instead of solving the equation of motion for $f(\mathbf{r}, \mathbf{k}, t)$ the method of moments is used to construct equations for expectation values of the form

$$\langle \Phi \rangle(\mathbf{r}, t) = \frac{1}{\underbrace{\int d^3k f(\mathbf{r}, \mathbf{k}, t)}_{=:n(\mathbf{r}, t)}} \int d^3k \Phi(\mathbf{k}) f(\mathbf{r}, \mathbf{k}, t). \quad (6)$$

This is done by multiplying eq. (1) by Φ and integration over d^3k . The result is

$$\frac{\partial}{\partial t} (n \langle \Phi \rangle) + \nabla_{\mathbf{r}} \cdot \mathbf{j}_{\langle \Phi \rangle} - n \mathbf{F}_{\langle \Phi \rangle} = \left(\frac{d}{dt} n \langle \phi \rangle \right)_{\text{coll}}, \quad (7)$$

with the *generalized current density* $\mathbf{j}_{\langle \Phi \rangle} = n \langle \mathbf{v} \otimes \Phi \rangle$ and the *generalized force* $\mathbf{F}_{\langle \Phi \rangle} = \mathbf{F} \cdot \langle \nabla_{\mathbf{k}} \otimes \Phi \rangle / \hbar$. Typically, the $\Phi(\mathbf{k})$ are low order polynomials in $v_x(\mathbf{k})$, $v_y(\mathbf{k})$ and $v_z(\mathbf{k})$, and the resulting equations (7) are of considerably simpler structure than the Boltzmann equation (1). However, starting with $\Phi(\mathbf{k}) \equiv 1$ eq. (7) generates an infinite hierarchy of equations (the *Boltzmann hierarchy*): the accounting equation for each *moment* $\langle \Phi \rangle$ contains the subsequent moment $\langle \mathbf{v} \otimes \Phi \rangle$ in the generalized current density. To obtain a finite closed system of equations it is necessary to terminate the hierarchy by dint of a phenomenological *ansatz*. For example, the hierarchy may be closed after the second moment $\Phi = \mathbf{v} \otimes \mathbf{v}$ by invoking the heat equation, $\mathbf{Q}_n = -\kappa \nabla_{\mathbf{r}} T_n$, to replace the non–convective contribution to the energy current (3rd order in \mathbf{v}) by quantities of lower order in \mathbf{v} .¹

2.1.2 Treatment of the scattering terms: the relaxation time approximation

Due to their inherently stochastic nature, the collision terms of the Boltzmann equation (1) are difficult to handle by deterministic methods. The same holds for the collision terms in the accounting equations (7)

$$\left(\frac{d}{dt} n \langle \Phi \rangle \right)_{\text{coll}} = n \left(\frac{d \langle \Phi \rangle}{dt} \right)_{\text{coll}} + \langle \Phi \rangle \underbrace{\left(\frac{dn}{dt} \right)_{\text{coll}}}_{=:G-R}; \quad (8)$$

¹Define the local electron temperature as $T_n = \frac{m_n}{3k_B} \text{Sp}(\mathbf{v} \otimes \mathbf{v})$.

$G - R$ is the change in local particle density due to interband (generation/recombination) processes.

The collision induced change in $\langle \phi \rangle$ is usually approximated by

$$\left(\frac{d \langle \Phi \rangle}{dt} \right)_{\text{coll}} \approx - \frac{\langle \Phi \rangle - \langle \Phi \rangle_{\text{eq}}}{\tau_{\langle \Phi \rangle}}, \quad (9)$$

with the *macroscopic relaxation time* $\tau_{\langle \Phi \rangle}$ and a suitably chosen *local equilibrium value* $\langle \Phi \rangle_{\text{eq}}$.

2.1.3 The classical semiconductor equations

Truncating the Boltzmann hierarchy after the second moment and applying the relaxation time approximation (4 different τ : momentum and energy relaxation times for both electrons and holes) together with the mobility equation $\mu = e\tau_{\mathbf{p}}/m^*$ and the *Einstein relations* ($D = k_B T / e\mu$) yields the equations of the *hydrodynamic model*. Under favorable conditions (*e.g.* not too large electric fields) additional assumptions may be made to simplify the hydrodynamic equations further:

- *Energy–balance equations* (neglect quadratic terms in \mathbf{j}),
- *Drift–diffusion equations* (local temperature of the carriers equal to the lattice temperature).

2.1.4 Classical non–locality of the transport parameters: Quasi–ballistic transport

Replacing the distribution function $f(\mathbf{r}, \mathbf{k}, t)$ by a few of its moments in $\mathbf{v}(\mathbf{k})$ abandons a large amount of information on the system. This poses some limits to the validity/applicability of the resulting models. For example, both the drift–diffusion equations and the hydrodynamic model contain a *mobility*. In devices with small electric fields and sufficiently strong scattering, the mobility may be parameterized in terms of local quantities (*e.g.* local electric field, local temperature)². In very small devices or in the presence of high electric fields, however, the mean electron velocity depends not only on local quantities, but acquires non–local dependences (velocity overshoot). This causes mobility–based transport models to loose their utility; consequently the Boltzmann equation needs to be solved directly.

Because of the high dimensionality of the space that harbors the distribution $f(\mathbf{r}, \mathbf{k}, t)$ and because of the stochastic nature of the collision term, Monte–Carlo methods seem to be best suited for the task. In ISE–TCAD this approach is available through the SPARTA module [6].

²Use bulk Monte–Carlo for computation.

2.2 Treatment of quantum–mechanical non–localities

In addition to the classical non–localities that arise under strong driving forces, when scattering processes are insufficient to restore equilibrium locally, quantum mechanics may cause small devices to exhibit non–local behavior even in equilibrium.

The Boltzmann equation and the semiconductor equations derived from it treat the electrons as though they were point particles (classical mass points). In quantum mechanics, however, an electron corresponds to an extended probability density distribution $|\psi|^2$, which (in single particle approximation) results from an eigensolution of the Schrödinger equation

$$\left(-\frac{\hbar^2}{2m^*}\nabla^2 + V(\mathbf{r})\right)\psi(\mathbf{r}) = E\psi(\mathbf{r}). \quad (10)$$

The term containing the Laplacian ∇^2 is a kinetic energy term. It causes localized wavefunctions ψ to have higher energies than extended wavefunctions. Or otherwise: given an energy E there is a minimum extension for the wavefunction ψ . In very small devices ($\lesssim 10$ nm in silicon; about 100 nm in GaAs [very small m^*]) this minimum extension becomes comparable with the extensions of the device; then, quantum–mechanics visibly alters the electrical properties of devices (*e.g.* conductance quantization [7]).

2.2.1 The density matrix and the quantum drift–diffusion model

The quantum mechanical generalization of the classical distribution function $f(\mathbf{r}, \mathbf{k}, t)$ is the *density matrix* ρ . Its time evolution is described by the Liouville equation

$$i\hbar\partial_t\rho = [\mathcal{H}, \rho]. \quad (11)$$

In position representation the density matrix takes the form

$$\rho = \int d^3r \int d^3r' |\mathbf{r}\rangle\rho(\mathbf{r}, \mathbf{r}')\langle\mathbf{r}'|. \quad (12)$$

By introducing center of mass $\bar{\mathbf{r}} = (\mathbf{r} + \mathbf{r}')/2$ and relative coordinates $\delta\mathbf{r} = \mathbf{r} - \mathbf{r}'$ and Fourier transforming $\rho(\bar{\mathbf{r}}, \delta\mathbf{r})$ with respect to the relative coordinate $\delta\mathbf{r}$ we obtain the *Wigner function* $f_W(\bar{\mathbf{r}}, \mathbf{k}, t)$.

The dynamic equation for the Wigner function is the *Wigner equation*. In its leading terms it is identical to the Boltzmann equation; but in addition it contains terms that contain 3rd and higher derivatives of the potential. Truncating the Wigner equation after the first additional term, applying the method of moments and closing the hierarchy by the equilibrium density matrix results in the *quantum drift–diffusion equations* (also known as *density gradient model*). [8]

2.2.2 Direct solution of the Wigner equation

The quantum drift–diffusion model is only valid close to equilibrium. Out of equilibrium it is liable to produce artifacts such as negative differential resistance [9]. This calls for direct solution of the Wigner equation. Unfortunately, the Wigner equation fraught with a negative sign problem, that renders Monte–Carlo methods for the Wigner equation much less efficient than for the Boltzmann equation and requires special treatment to achieve stability [10]. So far, direct solving of the Wigner equation is restricted to one–dimensional problems.

2.2.3 Coherent (ballistic) quantum transport

By ignoring coherence–breaking scattering processes, it is possible to construct a quantum mechanical transport model, that remains computationally tractable even for 2D/3D structures. We assume, that each terminal α of the device is coupled to an ideal thermal reservoir with an electro–chemical potential $\epsilon_F^{(\alpha)}$ (*cf.* fig. 1). Interactions

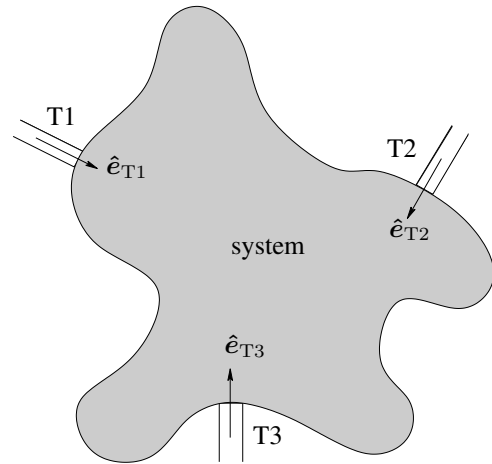


Figure 1: *The simulation domain (“system”) is coupled to the reservoirs by ideal waveguides.*

between the electrons are treated on the level of a mean field approach³. Under these circumstances, the stationary density matrix of the system becomes diagonal when expressed in the Kohn–Sham basis that results from imposing scattering boundary conditions at the terminals [11]

$$\rho = \sum_{\epsilon} \sum_{\alpha} \sum_i f\left(\frac{\epsilon_{\alpha,i} - \epsilon_F^{(\alpha)}}{k_B T}\right) |\epsilon, \alpha, i\rangle\langle\epsilon, \alpha, i|. \quad (13)$$

Here, ϵ is the energy of the state, α denotes the injecting terminal, and i is a collective label for the remaining quantum numbers. Then, the (particle) current through

³Actually a self–interaction reduced variant of LDA.

terminal α acquires the form

$$I_\alpha = \frac{1}{L} \frac{\hbar}{m} \int d\epsilon \left\{ f\left(\frac{\epsilon - \epsilon_F^{(\alpha)}}{k_B T}\right) \sum_i Z_{\alpha,i}^+(\epsilon) \times \right. \\ \times \left(1 - \sum_{i'} R_{(\alpha,i) \rightarrow (\alpha,i')}(\epsilon) \right) k_{\parallel,\alpha}^i(\epsilon) \\ \left. - \sum_{\beta \neq \alpha} f\left(\frac{\epsilon - \epsilon_F^{(\beta)}}{k_B T}\right) \sum_i Z_{\beta,i}^+(\epsilon) \times \right. \\ \left. \times \left(\sum_{i'} T_{(\beta,i) \rightarrow (\alpha,i')}(\epsilon) \right) k_{\parallel,\alpha}^i(\epsilon) \right\}, \quad (14)$$

with $Z_{\alpha,i}^+$ being the 1D density of (forward propagating) states of subband i in the waveguide connected to terminal α . The R and T terms are reflection and transmission probabilities connecting the indicated states.

For a two-terminal device without transverse structure (a true 1D device) the densities of states in both terminals are identical, and the current expression acquires Landauer-Büttiker shape⁴

$$I_{\rightarrow}^{1D} = \frac{2}{h} \int d\epsilon T(\epsilon) \left(f\left(\frac{\epsilon - \epsilon_F^{\rightarrow}}{k_B T}\right) - f\left(\frac{\epsilon - \epsilon_F^{\leftarrow}}{k_B T}\right) \right). \quad (15)$$

The quantum ballistic transport model has been implemented in the context of the SIMNAD quantum-mechanics simulator [12, 13]. The implementation is based on a multi-subband scattering matrix method [14]. In its restriction to non-interacting sub-bands, the formalism is equivalent to the ballistic limit of the non-equilibrium Green's function approach [15]. But whereas the NANOMOS simulator presented in [16] works in 1+1 dimensions (adiabatic decomposition), SIMNAD actually solves the full 2D/3D open Schrödinger equation in scattering configuration.

Figure 2 shows simulation results of SOI double gate MOSFETs with 1 nm body thickness and various gate lengths. We show results of quantum ballistic (2D-QB) transport calculations in two variants

- non self-consistent (nsc): the charge density is computed using 1D Schrödinger-Poisson; the scattering matrix formalism is invoked in a post-processing step to compute the current.
- self-consistent (sc): the scattering matrix formalism is used both for self-consistent computation of the charge density and for the current.

For comparison we also show results of drift-diffusion simulations using a 1D Schrödinger-Poisson charge density and the quantum-mechanical mobility model of [8]. Naturally, the assumption of ballistic transport leads to an over-estimation of the on-current; but the results on the blocking capabilities are predictive.

⁴In equation (14) a parabolic dispersion relation is assumed, but equation (15) remains valid in the non-parabolic case; see [11] for discussion.

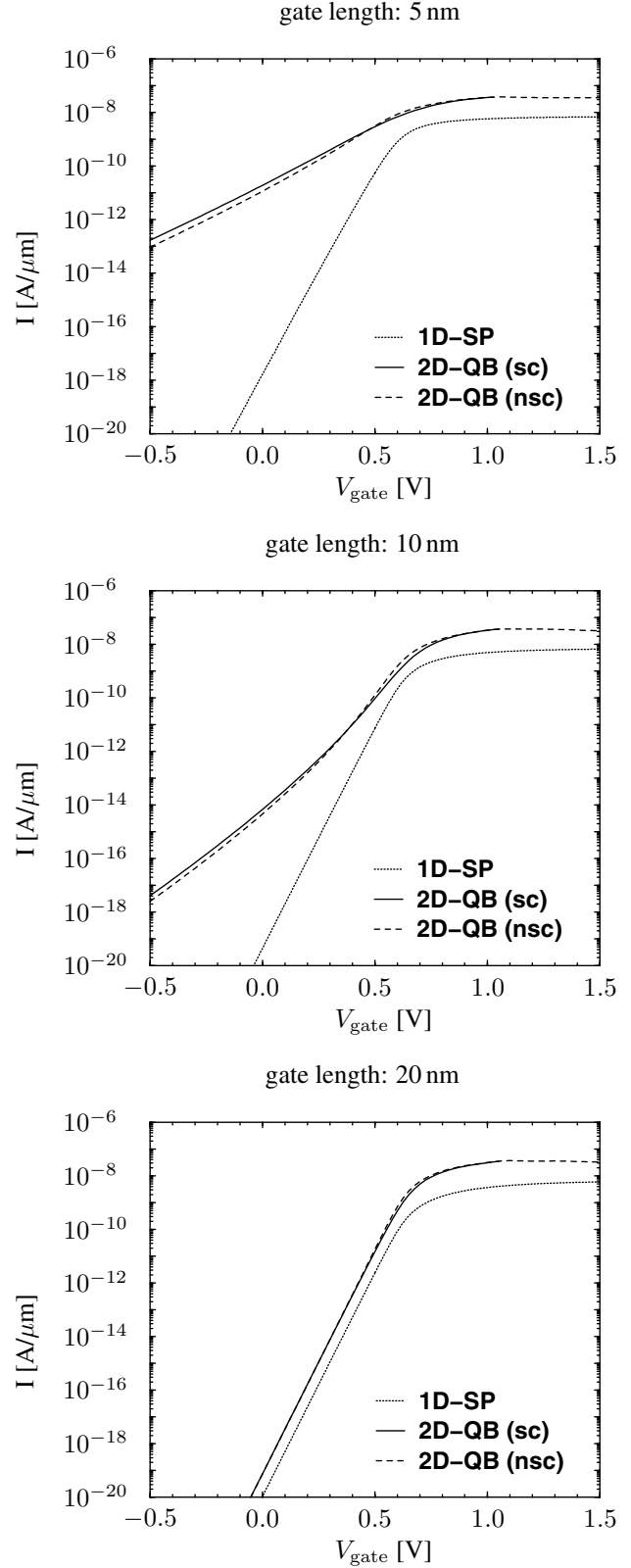


Figure 2: Transfer characteristics of SOI double gate MOSFETs by various models. $V_{\text{drain}} = 1 \mu\text{V}$. Silicon body thickness: 1 nm.

2.2.4 Particle interaction beyond mean field

In the first step of the derivation of the quantum ballistic transport model, it was assumed, that the electron–electron interaction could be treated by a mean field approach. This is typically a good assumption for spread-out wavefunctions. In systems with strongly localized wavefunctions (*e.g.* in the presence of quantum dots), however, this assumption may result in qualitatively wrong behavior: for example the assumption of Fermi–Dirac occupancy fails to produce Coulomb blockade effects (*cf.* fig. 3 and [11]). In such a situation the approach

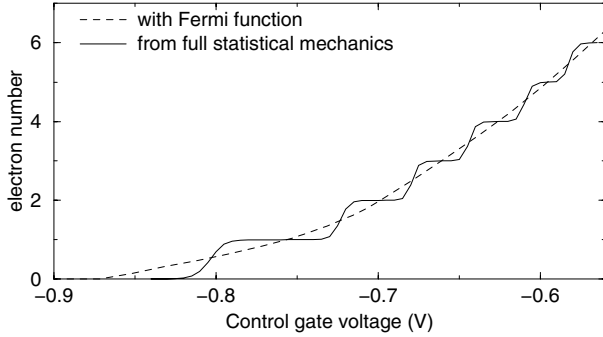


Figure 3: *Fermi statistics fails to produce the Coulomb charging staircase on the quantum dot of a single-electron transistor.*

used by SIMNAD is to decompose the grand canonical state of the quantum dot into its various canonical components (the grand canonical state is a statistical mixture of states with different total particle numbers N). A Kohn–Sham basis is computed for each canonical component (for this step Fermi–Dirac statistics with a shifted “effective” Fermi energy is assumed). For each canonical component the occupation factors of the Kohn–Sham orbitals as well as the free energy are computed by Monte–Carlo sampling of the restricted phase–space. The resulting free energies can be used to construct the grand canonical partition function and to obtain the probability by which each N –particle state enters into the grand canonical state.

3 Bridging the gap between conventional and nano–device simulation

Some candidate structures for future devices, especially for memory application, comprise both quantum dot regions and (semi–)classical channels. Up to now, such devices cannot be simulated with standard device simulators like DESSIS–ISE, because they cannot handle multidimensional confinement properly. SIMNAD, however, can do just this. On the other hand, SIMNAD does not contain any of the classical device models. By coupling both

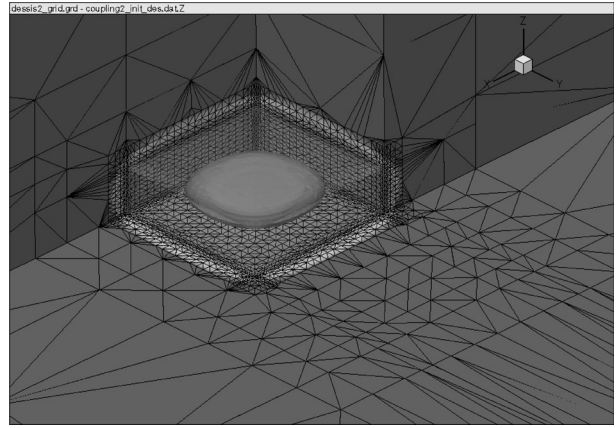


Figure 4: *The quantum–mechanical charge density has been transferred from SIMNAD to DESSIS–ISE.*

simulators self–consistently, we have obtained a simulation framework capable of addressing hybrid devices of the described type.

In this coupling scheme, DESSIS–ISE handles the total device geometry; SIMNAD only works on the sub-region inside which quantum confinement takes place. This choice is motivated through the fact, that DESSIS–ISE uses general Delaunay meshes, whereas SIMNAD operates on a tensor–product grid. Delaunay meshes are better suited for general geometries, but tensor–product grids have more structure, and allow for such mechanisms as dimensional reduction of the Schrödinger equation in situations in which there is strong confinement along some directions, while there is still classical behavior along the other directions.

Coupling two simulators, that operate on different grid types, raises the question of data exchange. In the original approach, the SIMNAD tensor product grid was incorporated into the Delaunay mesh used by DESSIS–ISE as a sub–mesh — this mesh merging is a service provided by `NOFFSET3D` [17, 18]. The advantage of this approach is the one–to–one correspondence between vertices in the quantum region of the merged DESSIS–ISE mesh and the SIMNAD grid. However, the resulting meshes tend to be very large. Also the merging procedure may conflict with mesh refinement requirements; and for some geometries embedding of the tensor product grid may be incompatible with the Delaunay condition.

These difficulties prompted us to revise the coupling strategy. The obvious alternative is maintaining separate grids for each simulator. This introduces the need to interpolate data during transfer; but contrary to our misgivings, this did not compromise convergence — the self–consistent solution of the Kohn–Sham equations took the same number of iterations regardless if both the Kohn–Sham and Poisson’s equation were solved by SIMNAD or if Poisson’s equation was handled by DESSIS–ISE.

Figure 4 depicts the quantum mechanical charge density inside the quantum dot, as it has been handed over

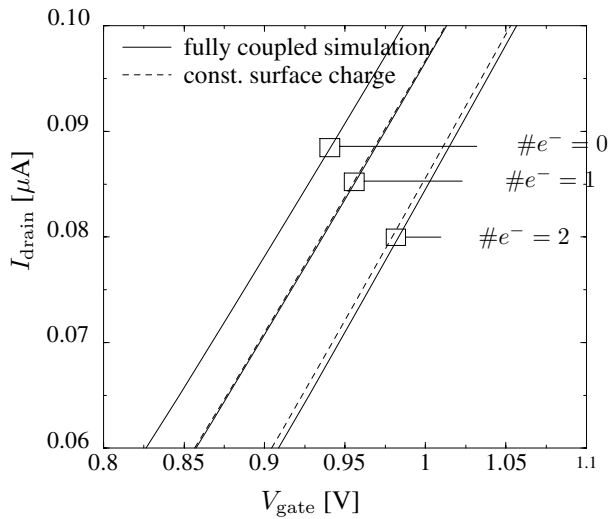


Figure 5: Transfer characteristics of the modified nano-flash device; comparison of I - V curves obtained with a constant surface charge density (dashed) and fully coupled simulations with self-consistent polarisation of the quantum-mechanical charge density (solid).

from SIMNAD to DESSIS-ISE. Figure 5 shows simulated transfer characteristics of the channel underneath the floating gate. Dashed curves were computed with the assumption that the quantum dot charge is homogeneously spread over the surface of the quantum dot; solid curves are results of self-consistently coupled DESSIS-ISE/SIMNAD simulations with the 3D quantum-mechanical SIMNAD charge density arranging itself in each iteration inside the potential supplied by DESSIS-ISE.

4 Conclusion

The scaling requirements of the ITRS Roadmap are driving semiconductor devices to length scales on which classical and quantum non-local effects become significant. This calls for simulation tools capable of including these effects. In this paper we have proposed ways to move from conventional device modeling towards the modeling of nano-devices. In this regime the predictivity of standard device modeling is not yet achieved, but the situation is continuously improving.

Acknowledgment

One of the authors (F.H.) wishes to thank Bernhard Schmithüsen for his implementation work on the DESSIS-ISE side of the simulator coupling.

References

- [1] Gordon E. Moore. Cramming more components onto integrated circuits. *Electronics*, 38(8), 1965.
- [2] International technology roadmap for semiconductors. published online at <http://public.itrs.net>, 2003.
- [3] Ludwig Boltzmann. Weitere Studien ueber das Waermegleichgewicht unter Gasmolekuelen. *Sitzungsberichte der Oesterreichischen Akademie der Wissenschaften*, 76:275–370, 1872.
- [4] Neil W. Ashcroft and N. David Mermin. *Solid State Physics*. Saunders College Publishing, Harcourt Brace College Publishers, Forth Worth, Philadelphia, San Diego, New York, Orlando, Austin, San Antonio, Toronto, Montreal, London, Sydney, Tokyo, 1976.
- [5] K. Bløtekjær. Transport equations for electrons in two-valley semiconductors. *IEEE Trans. Elec. Dev.*, 17:38–47, 1970.
- [6] F. M. Bufler, C. Zechner, A. Schenk, and W. Fichtner. Single-particle approach to self-consistent Monte Carlo device simulation. *IEICE Trans. Electron.*, E86-C:308–313, 2003.
- [7] B. J. van Wees, L. P. Kouwenhoven, E. M. M. Williams, C. J. P. M. Harmans, J. E. Mooij, C. W. J. von Houten, C. W. J. Beenakker, J. G. Williamson, and C. T. Foxen. Quantum ballistic and adiabatic electron transport studied with quantum point contacts. *Phys. Rev. B*, 43(15), 1991.
- [8] Andreas Wettstein. *Quantum Effects in MOS Devices*. PhD thesis, ETH Zürich, published at Hartung Gorre Verlag, Konstanz; ISBN 3-89649-566-6, 2000.
- [9] Timm Höhr, Andreas Schenk, Andreas Wettstein, and Wolfgang Fichtner. On density-gradient modeling of tunneling through insulators. *IEICE Trans. Electron.*, E86-C:379–384, 2003.
- [10] H. Kosina, M. Nedjalkov, and S. Selberherr. A Monte-Carlo method seamlessly linking quantum and classical transport calculations. *J. Comput. Electron.*, 2:147–151, 2003.
- [11] Frederik Ole Heinz. *Simulation Approaches for Nanoscale Semiconductor Devices*. PhD thesis, ETH Zürich, published at Hartung Gorre Verlag, Konstanz; ISBN 3-89649-910-6, 2004.
- [12] Andreas Scholze, Andreas Schenk, and Wolfgang Fichtner. Single-electron device simulation. *IEEE Trans. Electron Devices*, 47(10):1811–1818, 2000.
- [13] Frederik Ole Heinz. *Users' Manual: SIMNAD, a Simulator for Nano Devices*. ETH Zürich, 2003.
- [14] David Yuk Kei Ko and J. C. Inkson. Matrix method for tunneling in heterostructures: Resonant tunneling in multilayer systems. *Phys. Rev. B*, 38(14):9945–9951, 1988.

- [15] Supriyo Datta. Nanoscale device modeling: the Green's function method. *Superlattices and Microstructure*, 28(4):253–278, 2000.
- [16] Zhibin Ren, Ramesh Venagupal, Sebastien Goasguen, Supriyo Datta, and Mark S. Lundstrom. nanoMOS 2.5: A two-dimensional simulator for quantum transport in double-gate MOSFETs. *IEEE Trans. Elec. Dev.*, 50(9):1914–1925, 2003.
- [17] ISE AG Zürich. '*ISE TCAD Manuals*', Release 8.0, volume 4a, 2002.
- [18] Jens Krause. *On boundary conforming anisotropic Delauney meshes*. PhD thesis, ETH Zürich, published at Hartung Gorre Verlag, Konstanz, 2001.